SCIENCE CHINA
Information Sciences

• RESEARCH PAPER •

January 2026, Vol. 69, Iss. 1, 112201:1–112201:14
https://doi.org/10.1007/s11432-024-4368-3

Distributed cooperative learning control for multiagent systems with data protection and disturbance observation

Min WANG[1], Xiao-Jie PENG[1*], Hongyi LI[1] & Yong HE[2]

[1]*College of Electronic and Information Engineering, Southwest University, Chongqing 400715, China*
[2]*School of Automation, China University of Geosciences, Wuhan 430074, China*

Received 30 September 2024/Revised 23 December 2024/Accepted 25 March 2025/Published online 10 September 2025

Abstract This paper presents a distributed cooperative learning control strategy that incorporates data protection and a disturbance observer. Specifically, an encryption-decryption mechanism is proposed through the construction of mask functions and command filtering. This mechanism not only protects agent information from being exposed but also reduces the impact on system performance caused by the mask function. Additionally, a self-correction mechanism with an amendment function is proposed for the disturbance observer, addressing the issue of error over-compensation. Furthermore, neighbor information is incorporated into the adaptive law to enhance the robustness of system. The designed trigger condition accounts for the effects of trigger errors and system tracking performance, effectively conserving communication resources while maintaining system performance. Finally, the simulation results validate the theoretical findings.

Keywords cooperative learning, encryption-decryption mechanism, external disturbances, mask function, multiagent systems

Citation Wang M, Peng X-J, Li H Y, et al. Distributed cooperative learning control for multiagent systems with data protection and disturbance observation. Sci China Inf Sci, 2026, 69(1): 112201, https://doi.org/10.1007/s11432-024-4368-3

1 Introduction

As an emerging research area, security control [1–5] has attracted considerable attention owing to the inherent risks associated with information exchange. To mitigate concerns regarding privacy information leakage, extensive efforts have been made to address this challenge. For instance, Liu et al. [6] protected agent privacy using the differential privacy method, which achieved protection by introducing random noise. Alternatively, the time-varying output mask function [7–10] was used to protect agent information without relying on stochastic noise. An encryption-decryption scheme [11] was proposed to prevent information leakage during communication. For nonlinear 2-D shift-varying systems [12], a logarithmic-type encoding-decoding mechanism was implemented for each individual sensor node, incorporating an optimization scheme. Although strategies [6–12] effectively protect data, they can also impact subsequent control strategies, potentially causing deviations from the intended control objectives. In other words, while the system is operating, the abovementioned schemes still have an adverse effect on system performance. Given the need to minimize this impact, protecting the sensitive information of agents is a worthwhile area of research.

Because unknown functions are inevitable in most real system models [13–15], neural networks and fuzzy logic systems, which effectively handle unknown functions, have gained considerable attention. As research progresses, a new approach based on neural network technology [16, 17] was proposed to enhance the robustness of control strategies, known as the cooperative learning strategy. The cooperative learning strategy [18, 19] is defined as a method for promoting knowledge sharing across the network, incorporating neighbor weight information into adaptive laws. Building on this, several results have emerged [20,21]. Yuan et al. [20] introduced an innovative formation control scheme with cooperative deterministic learning, leveraging neural networks. The distributed cooperative adaptive neural network controller proposed in [21] demonstrated exceptional capabilities in identifying and learning system dynamics cooperatively along the trajectories of all agents in the network, while also incorporating error adjustment. Based on these theoretical contributions [18,20,21], numerous researchers have further investigated the impact of communication burden on cooperative learning. Gao et al. [22] proposed distributed cooperative learning laws incorporating an event-triggered strategy to reduce communication overhead. For a team of hypersonic flight

* Corresponding author (email: xjpeng@swu.edu.cn)

vehicles [23], an event-triggered distributed containment control scheme based on learning was developed, using a switching threshold strategy for communication between different hypersonic flight vehicles. However, in constructing trigger conditions, the approaches in [22,23] considered only the trigger error, whereas communication resources should not be conserved at the cost of system performance. This motivated the research in this paper to propose an event-triggered cooperative learning control strategy that considers trigger error and system performance.

Beyond designing a cooperative learning control strategy to maintain system dynamics, the influence of external disturbances [24, 25] cannot be overlooked because accounting for them enhances the reliability of the proposed control strategy. To mitigate the effects of external disturbances, disturbance observers with strong disturbance estimation capabilities have gained considerable attention. In [26], multiple disturbances were effectively managed using a disturbance observer, improving estimation accuracy. Similarly, Kong et al. [27] developed a disturbance observer to handle external disturbances originating from exogenous systems. With the widespread application and continuous advancement of disturbance observers, many researchers have extended their fundamental capabilities. In [28], a disturbance observer with high-accuracy disturbance estimation was proposed. To mitigate the effects of unmodeled disturbances on estimation in [29], the sliding mode technique was integrated into the disturbance observer. Beyond these theoretical contributions [26–29], ensuring control accuracy remains a critical research direction, especially for practical applications. Furthermore, developing an effective self-correction mechanism based on the disturbance observer is essential to enhance system tracking performance while addressing the issue of over-compensation during the design process.

In summary, this paper presents a scheme that enhances data protection and control performance from the perspective of cooperative learning. This is achieved by developing a data-driven encryption-decryption mechanism and a self-correction mechanism for the disturbance observer. The main contributions can be summarized as follows.

(1) An encoding-decoding mechanism is proposed by constructing encoding functions and a command filtering strategy. Specifically, the impact on system control performance is mitigated by compensating for the encryption function.

(2) Drawing inspiration from the gradient descent method, a self-correction mechanism with an amendment function is introduced for the disturbance observer. This mechanism addresses the issue of over-compensation in tracking performance and helps reduce it to some extent.

(3) An improved event-triggered cooperative learning strategy is designed to enhance the robustness of the system by incorporating neighbor weight information. Unlike existing work [23], the constructed trigger condition considers both the trigger error and the control performance of the system by introducing the corresponding error. This approach minimizes unnecessary communication burden while ensuring performance.

Notation. diag$(\cdot)$ denotes a the diagonal matrix. $\mathbb{R}^s$ and $\mathbb{R}^n$ represent s and n-dimensional real vectors, respectively. csch$(\cdot)$ is the hyperbolic cosecant function.

2 Preliminaries

2.1 Graph theory

A graph [30] $\mathbb{G} = (\mathbb{V}, \mathbb{E}, \mathbb{A})$ represents the data transfer relationships between agents. The set of nodes is given by $\mathbb{V} = (1, \ldots, N)$, and the edge set is $\mathbb{E} \subseteq \mathbb{V} \times \mathbb{V}$. The set of neighbors for agent i is defined as $H_i = \{\mathbb{V}_j | (\mathbb{V}_j, \mathbb{V}_i) \in \mathbb{E}, i \neq j\}$. The adjacency matrix is denoted as $\mathbb{A} = [a_{ij}]$, where a_{ij} indicates that agent j transmits data to agent i. The diagonal matrix is given by $\mathbb{D} = \text{diag}(d_1, \ldots, d_N)$ with $d_i = \sum_{j=1}^{N} a_{ij}$, and the Laplacian matrix is defined as $\mathbb{L} = \mathbb{D} - \mathbb{A}$.

Assumption 1 ([31–34])**.** The graph $\mathbb{G}$ contains a spanning tree with the leader node 0 as the root.

2.2 Problem formulation

Consider the ith $(i = 1, \ldots, N)$ nonlinear strict-feedback multiagent system

$$\begin{cases} \dot{x}_{i,s} = x_{i,s+1} + \varphi_{i,s}(\breve{x}_{i,s}) + \breve{D}_{i,s}, & 1 \leqslant s \leqslant n-1, \\ \dot{x}_{i,n} = \mathfrak{u}_i + \varphi_{i,n}(\breve{x}_{i,n}) + \breve{D}_{i,n}, \\ y_i = x_{i,1}, \end{cases} \tag{1}$$

where $\breve{x}_{i,\bullet} = [x_{i,1}, \ldots, x_{i,\bullet}]^{\mathrm{T}} \in \mathbb{R}^{\bullet}$ is the state vector. $\varphi_{i,\bullet}(\breve{x}_{i,\bullet})$, $u_i \in \mathbb{R}$ and $y_i \in \mathbb{R}$ denote unknown function, the control input and the output signal, respectively. The terms $\breve{D}_{i,s}$ and $\breve{D}_{i,n}$ denote bounded external disturbances.

Assumption 2 ([35]). The leader signal $y_c(t)$ and its nth order derivative y_c^n are bounded and continuously differentiable.

The synchronization error is defined as

$$z_{i,1} = \sum_{j=1}^{N} a_{ij}(y_i - y_j) + b_i(y_i - y_c). \tag{2}$$

Lemma 1 ([36]). Under Assumption 1, $\mathbb{L} + \mathbb{B}$ is nonsingular, where $\mathbb{B} = \mathrm{diag}\{b_i\}$, and b_i represents the weight between the leader and the followers.

Lemma 2 ([36]). Define $\acute{z}_{i,1} = (z_{1,1}, \ldots, z_{N,1})^{\mathrm{T}}$, $\acute{y} = (y_1, \ldots, y_N)^{\mathrm{T}}$, $\acute{y}_c = (y_c, \ldots, y_c)^{\mathrm{T}}$. Then, it follows that

$$\|\acute{y} - \acute{y}_c\| \leqslant \frac{\|\acute{z}_{i,1}\|}{\ell(\mathbb{L} + \mathbb{B})}, \tag{3}$$

where $\ell(\mathbb{L} + \mathbb{B})$ denotes the minimum singular value of $\mathbb{L} + \mathbb{B}$.

Fuzzy logic systems (FLSs). FLSs are introduced to handle the unknown function $\varphi_{i,\flat}(x)$. For any $\epsilon_{i,\flat} > 0$, it follows that

$$\sup_{x \in \Omega} |\varphi_{i,\flat}(x) - \vartheta_{i,\flat}^{*\mathrm{T}} \Xi_{i,\flat}(x)| \leqslant \epsilon_{i,\flat}, \tag{4}$$

where $\vartheta_{i,\flat}^*$ is the weight vector, given by $\vartheta_{i,\flat}^* = [\vartheta_{i,\flat 1}^*, \ldots, \vartheta_{i,\flat s}^*]^{\mathrm{T}}$, with s as the number of rules. $\Xi_{i,\flat}(x)$ represents the basis function vector, and Ω is a compact set. The term $\bar{\epsilon}_{i,\flat}$ is a positive constant satisfying $|\epsilon_{i,\flat}| \leqslant \bar{\epsilon}_{i,\flat}$.

Lemma 3 ([37,38]). The command filtering is designed as

$$\upsilon_{i,s}\dot{\bar{\alpha}}_{i,s} + \bar{\alpha}_{i,s} = \alpha_{i,s-1}, \bar{\alpha}_{i,s}(0) = \alpha_{i,s-1}(0), \ s = 2, \ldots, n, \tag{5}$$

where $\upsilon_{i,s}$ is a positive constant, and $\bar{\alpha}_{i,1} = y_c$ represents the output of the first-order command filtering.

Lemma 4 ([37]). For $\vec{\kappa}_{i,p} \in \mathbb{R}^+$ and $\xi_{i,p} \in \mathbb{R}$, the following inequality holds:

$$|\xi_{i,p}| - \frac{\xi_{i,p}^2}{\sqrt{\xi_{i,p}^2 + \vec{\kappa}_{i,p}^2}} \leqslant \vec{\kappa}_{i,p}. \tag{6}$$

Control goal. The objective is to construct a distributed cooperative learning control scheme that ensures the following:

(1) All signals in the closed-loop system are semi-globally uniformly ultimately bounded (SGUUB);

(2) The synchronization error converges to a small neighborhood near the origin.

2.3 Encoding-decoding mechanism

The goal of the proposed encoding-decoding mechanism is to protect the data of the agent from leakage while minimizing its impact on tracking performance. To protect the sensitive information of the agent, the following encryption function has been established.

$$\hbar_{i,\flat} = \begin{cases} \breve{\iota}_{i,\flat} \mathrm{e}^{\iota_{i,\flat}(T_{i,\flat} - t)}, & t \leqslant T_{i,\flat}, \\ \breve{\iota}_{i,\flat} \aleph_{i,\flat}^{\frac{\iota_{i,\flat}(T_{i,\flat} - t)}{\ln \aleph_{i,\flat}}}, & t > T_{i,\flat}, \end{cases} \tag{7}$$

where $\iota_{i,\flat}$, $\breve{\iota}_{i,\flat}$ and $\aleph_{i,\flat}$ are positive constants with $\aleph_{i,\flat} > e$ and $\flat = 1, 2, \ldots, n$. $T_{i,\flat}$ is the time that the user can arbitrarily adjust. $\hbar_{i,\flat}$ is the encryption function, which is monotonically decreasing, and the variable $\hbar_{i,\flat}$ tends to 0 as time approaches infinity. Specifically, $\lim_{t \to T_{i,\flat}^-} \breve{\iota}_{i,\flat} \mathrm{e}^{\iota_{i,\flat}(T_{i,\flat} - t)} = \lim_{t \to T_{i,\flat}^+} \breve{\iota}_{i,\flat} \aleph_{i,\flat}^{\frac{\iota_{i,\flat}(T_{i,\flat} - t)}{\ln \aleph_{i,,\flat}}}$ and $\lim_{t \to \infty} \hbar_{i,\flat} = 0$. Furthermore, according to (7), the user can change the encryption function to another function as soon as time reaches $T_{i,\flat}$ because the constructed encryption function is a segmented function.

Remark 1. It is important to note that most studies on the construction of encryption functions [7–9] involve continuous time-varying functions. In contrast, the proposed encryption function is a piecewise continuous function, which enhances the encryption ability of the sensitive information for the agents because the user can modify the encryption function at any time.

Algorithm 1 Encryption mechanism.

Require: $x_{i,\flat}$, $\hbar_{i,\flat}$.
  if $t \in [0, T_{i,\flat}]$ **then**
    $\beta_{i,\flat} = x_{i,\flat} + \breve{\iota}_{i,\flat} \mathrm{e}^{\iota_{i,\flat}(T_{i,\flat}-t)}$;
  else
    $\beta_{i,\flat} = x_{i,\flat} + \breve{\iota}_{i,\flat} \aleph_{i,\flat}^{\frac{\iota_{i,\flat}(T_{i,\flat}-t)}{\ln \aleph_{i,\flat}}}$;
  end if
Ensure: $\beta_{i,\flat}$.

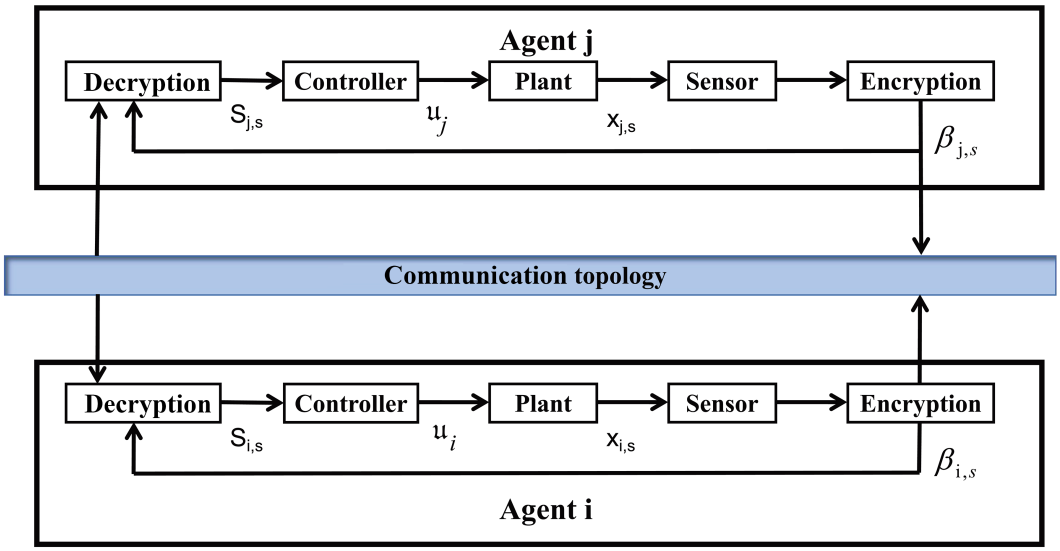

Figure 1 (Color online) Diagram of the encoding-decoding mechanism.

The state of the agent with an encryption function can be expressed as

$$\beta_{i,\flat} = x_{i,\flat} + \hbar_{i,\flat}. \tag{8}$$

By incorporating the encryption function $\hbar_{i,\flat}$ in the state information $x_{i,\flat}$, the converted signal $\beta_{i,\flat}$ diverges from the original state information $x_{i,\flat}$, thereby protecting the state information of agents.

Additionally, different encryption functions can be assigned to individual agents, and the time $T_{i,\flat}$ at which the encryption functions are transformed can be freely chosen. Moreover, this paper focuses on the protection of state information for all agents, enhancing the encryption capacity of the control system through these measures.

Building on this, an encryption mechanism with a flexible encryption function is developed to protect the sensitive information of agents. This encryption mechanism is outlined in Algorithm 1.

Meanwhile, the decryption function is

$$\breve{\hbar}_{i,\flat} = \frac{\breve{w}_{i,\flat}}{\breve{w}_{i,\flat} + \breve{\upsilon}_{i,\flat} \mathrm{e}^{-\nabla_{i,\flat} t}}, \tag{9}$$

where $\breve{w}_{i,\flat}$, $\breve{\upsilon}_{i,\flat}$ and $\nabla_{i,\flat}$ are positive parameters. The decryption function (9) can control the speed at which the encrypted information is restored to its original form. Specifically, the restoration tendency of the decryption function can be either accelerated or slowed down. The decryption process will be discussed further below.

Remark 2. By adjusting the parameters $\breve{\upsilon}_{i,\flat}$ and $\nabla_{i,\flat}$ in (9) and combining them with the encryption function, the speed at which the true data are restored can be controlled.

Remark 3. In the decryption process shown in Figure 1, the proposed strategy does not directly recover the original data, but instead gradually restores it. This approach effectively protects the sensitive information of the agent from being exposed.

Furthermore, the equation of the system can be transformed into

$$\begin{cases} \dot{\beta}_{i,s} = \beta_{i,s+1} + \varphi_{i,s}(\breve{x}_{i,s}) + \dot{\hbar}_{i,s} + \breve{D}_{i,s}, \quad 1 \leqslant s \leqslant n-1, \\ \dot{\beta}_{i,n} = \mathrm{u}_i + \varphi_{i,n}(\breve{x}_{i,n}) + \dot{\hbar}_{i,n} + \breve{D}_{i,n}, \\ \acute{y}_i = \beta_{i,1}, \end{cases} \tag{10}$$

Algorithm 2 Amendment mechanism.

Require: $|\frac{\partial\dot{\hat{\nu}}_{i,\flat k}}{\partial\chi_{i,\flat k}} - \frac{\partial\dot{\hat{\nu}}_{i,\flat(k-1)}}{\partial\chi_{i,\flat(k-1)}}|$, $|\frac{\partial\dot{\hat{\nu}}_{i,\flat k}}{\partial\chi_{i,\flat k}}|$.
  if $|\frac{\partial\dot{\hat{\nu}}_{i,\flat k}}{\partial\chi_{i,\flat k}} - \frac{\partial\dot{\hat{\nu}}_{i,\flat(k-1)}}{\partial\chi_{i,\flat(k-1)}}| < |\frac{\partial\dot{\hat{\nu}}_{i,\flat k}}{\partial\chi_{i,\flat k}}|$ **then**
    $\jmath_{i,\flat k} = |\frac{\partial\dot{\hat{\nu}}_{i,\flat k}}{\partial\chi_{i,\flat k}} - \frac{\partial\dot{\hat{\nu}}_{i,\flat(k-1)}}{\partial\chi_{i,\flat(k-1)}}|$;
  else
    $\jmath_{i,\flat k} = |\frac{\partial\dot{\hat{\nu}}_{i,\flat k}}{\partial\chi_{i,\flat k}}|$;
  end if
Ensure: $\jmath_{i,\flat k}$.

where $\beta_{i,s}$ is the state variable with the encryption function. Based on the system model (1), the encryption function is integrated into the system's state variable. After a series of transformations, the system model (1) is ultimately reorganized as system model (10). Therefore, system model (10) represents a secure system that incorporates encrypted data.

2.4 Disturbance observer

A disturbance observer with self-correction is designed to estimate the external disturbance $\breve{D}_{i,\flat}$. First, assume that the external disturbance $\breve{D}_{i,\flat}$ in model (1) is generated by an exogenous system [27], which is expressed as

$$\begin{cases} \dot{\tau}_{i,\flat} = G_{i,\flat}\tau_{i,\flat} + \Psi_{i,\flat}, \\ \breve{D}_{i,\flat} = \eta_{i,\flat}\tau_{i,\flat}, \end{cases} \tag{11}$$

where $G_{i,\flat}$ and $\eta_{i,\flat}$ are constants. Meanwhile, assume that the state variable $\tau_{i,\flat}$ and the unknown function $\Psi_{i,\flat}$ are bounded. Define the auxiliary variables $\nu_{i,\flat} = \tau_{i,\flat} - \mu_{i,\flat}\beta_{i,\flat}$, where $\mu_{i,\flat}$ is a constant.

According to (10) and (11), the derivative of $\nu_{i,\flat}$ is

$$\dot{\nu}_{i,\flat} = (G_{i,\flat} - \mu_{i,\flat}\chi_{i,\flat}\eta_{i,\flat})\nu_{i,\flat} + \zeta_{i,\flat} + \varpi_{i,\flat}, \tag{12}$$

where $\zeta_{i,\flat} = \Psi_{i,\flat} + \mu_{i,\flat}\chi_{i,\flat}\breve{D}_{i,\flat}$ and $\varpi_{i,\flat} = (G_{i,\flat} - \mu_{i,\flat}\chi_{i,\flat}\eta_{i,\flat})\mu_{i,\flat}\beta_{i,\flat} - \mu_{i,\flat}\dot{\beta}_{i,\flat}$. Inspired in part by [27], it can be inferred that $\zeta_{i,\flat}$ is bounded with $|\zeta_{i,\flat}| \leqslant \vec{\zeta}_{i,\flat}$, where $\vec{\zeta}_{i,\flat}$ represents a constant, and $\dot{\beta}_{i,\flat}$ is available. $\chi_{i,\flat}$ is the constructed self-correction mechanism, which can improve the control precision.

The disturbance observer with self-correction is constructed as

$$\hat{\breve{D}}_{i,\flat} = \eta_{i,\flat}[\hat{\nu}_{i,\flat} + \mu_{i,\flat}\beta_{i,\flat}], \tag{13}$$

$$\dot{\hat{\nu}}_{i,\flat} = (G_{i,\flat} - \mu_{i,\flat}\chi_{i,\flat}\eta_{i,\flat})\hat{\nu}_{i,\flat} + \varpi_{i,\flat}, \tag{14}$$

where $|\frac{G_{i,\flat}+\frac{1}{2}}{\eta_{i,\flat}}| < \chi_{i,\flat} < \vec{\chi}_{i,\flat}$, and $\vec{\chi}_{i,\flat}$ is a constant.

Remark 4. Various effective methods exist for handling disturbances, including setting limits to disturbances, and constructing sliding mode disturbance observers [39,40]. The choice of a specific disturbance-handling approach should align with the objectives of the study.

To mitigate disturbances within a fixed time frame, the fixed-time sliding mode disturbance observer [40] is a highly effective option. In this paper, to address disturbances while ensuring the control performance of the system, the disturbance observer (13) is constructed.

A detailed self-correction mechanism to mitigate the over-compensation for errors is shown in Algorithm 2.

To ensure high-precision control, the self-correction mechanism with an amendment function is constructed as

$$\chi_{i,\flat k} = \chi_{i,\flat(k-1)} - \jmath_{i,\flat k}\mathrm{sgn}(S_{i,\flat k})\mathrm{sgn}\left(\frac{\partial\dot{\hat{\nu}}_{i,\flat k}}{\partial\chi_{i,\flat k}}\right)\mathrm{sgn}\left(\frac{\partial\dot{S}_{i,\flat k}}{\partial\hat{\nu}_{i,\flat k}}\right), \tag{15}$$

where the negative gradient terms are defined as $\frac{\partial\dot{\hat{\nu}}_{i,sk}}{\partial\chi_{i,sk}} = -\eta_{i,sk}\mu_{i,sk}\hat{\nu}_{i,sk}$, $\frac{\partial\dot{\hat{\nu}}_{i,1k}}{\partial\chi_{i,1k}} = -\eta_{i,1k}\mu_{i,1k}\hat{\nu}_{i,1k}$, $\frac{\partial\dot{S}_{i,1k}}{\partial\hat{\nu}_{i,1k}} = -\delta_i\eta_{i,1k}$ and $\frac{\partial\dot{S}_{i,sk}}{\partial\hat{\nu}_{i,sk}} = -\eta_{i,sk}$ with $\delta_i = (d_i + b_i)$. The transformed error $S_{i,s}$ is given by $\dot{S}_{i,1} = \delta_i[z_{i,2} + \bar{\alpha}_{i,2} - \alpha_{i,1} - k_{i,1}S_{i,1} - q_{i,1}S_{i,1} - k_{i,1}\xi_{i,1} - \frac{\ell_{i,1}\xi_{i,1}}{\sqrt{\xi_{i,1}^2+\sigma_{i,1}^2}} - \frac{1}{\delta_i}\hat{\vartheta}_{i,1}^{\mathrm{T}}\Xi_{i,1} - \hat{\breve{D}}_{i,1} + \frac{\sum_{j=1}^{N}a_{ij}}{\delta_i}(\beta_{j,2} + \hat{\breve{D}}_{j,1}) + \frac{b_i}{\delta_i}\dot{y}_c + \varphi_{i,1} + \dot{\hbar}_{i,1} + \breve{D}_{i,1}] - \sum_{j=1}^{N}a_{ij}[\beta_{j,2} + \varphi_{j,1} + \dot{\hbar}_{j,1} + \breve{D}_{j,1}] - b_i(y_r)' - \dot{\xi}_{i,1}$. The detailed construction process is provided in later sections.

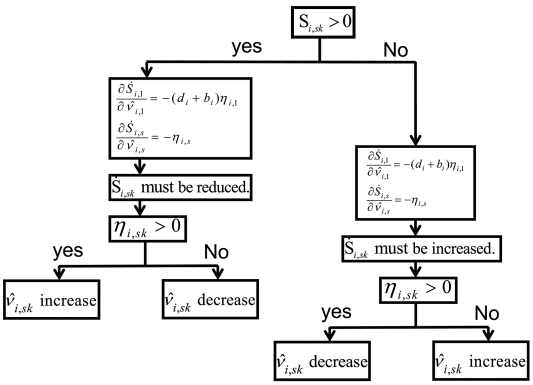

Figure 2 Iterative process in the self-correction mechanism (the relationship between $S_{i,sk}$ and $\hat{v}_{i,sk}$).

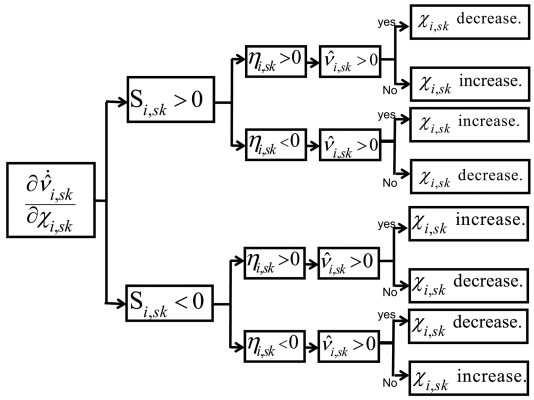

Figure 3 Iterative process in the self-correction mechanism (the relationship between $\hat{v}_{i,sk}$ and $\chi_{i,sk}$).

Remark 5. In situations involving error over-compensation, the proposed self-correction mechanism helps mitigate the issue to some extent.

Algorithm 2 is designed to minimize error offset by comparing the values of $|\frac{\partial \dot{\hat{\nu}}_{i,\flat k}}{\partial \chi_{i,\flat k}} - \frac{\partial \dot{\hat{\nu}}_{i,\flat(k-1)}}{\partial \chi_{i,\flat(k-1)}}|$ and $|\frac{\partial \dot{\hat{\nu}}_{i,\flat k}}{\partial \chi_{i,\flat k}}|$. Unlike conventional self-correction mechanisms that consider only the negative gradient at each step, the proposed mechanism evaluates the difference between the current and previous negative gradients. This approach helps mitigate the issue of over-compensation, where excessive error correction may lead to instability.

Inspired by the gradient descent method, the core idea of the self-correction mechanism with the amendment function is to ensure that the error converges to zero under all circumstances. Detailed instructions are provided below.

When $S_{i,sk} > 0$, for $S_{i,sk}$ to converge to zero more effectively, $\dot{S}_{i,sk}$ must decrease. The details are as follows. Based on $\frac{\partial \dot{S}_{i,1k}}{\partial \dot{\hat{\nu}}_{i,1k}} = -\delta_i \eta_{i,1k}$ and $\frac{\partial \dot{S}_{i,sk}}{\partial \dot{\hat{\nu}}_{i,sk}} = -\eta_{i,sk}$, $\hat{\nu}_{i,sk}$ should increase if $\eta_{i,sk} > 0$; otherwise, $\hat{\nu}_{i,sk}$ should decrease if $\eta_{i,sk} < 0$. Therefore, the self-correction mechanism $\chi_{i,sk}$ is designed to ensure that $\hat{\nu}_{i,sk}$ consistently moves toward the optimal state.

When $S_{i,sk} < 0$, for $S_{i,sk}$ to converge to zero more effectively, $\dot{S}_{i,sk}$ must increase. The details are as follows. Based on $\frac{\partial \dot{S}_{i,1k}}{\partial \dot{\hat{\nu}}_{i,1k}} = -\delta_i \eta_{i,1k}$ and $\frac{\partial \dot{S}_{i,sk}}{\partial \dot{\hat{\nu}}_{i,sk}} = -\eta_{i,sk}$, $\hat{\nu}_{i,sk}$ should decrease if $\eta_{i,sk} > 0$; otherwise, $\hat{\nu}_{i,sk}$ should increase if $\eta_{i,sk} < 0$. Therefore, the self-correction mechanism $\chi_{i,sk}$ is designed to ensure that $\hat{\nu}_{i,sk}$ consistently moves toward the optimal state.

A thorough analysis of the thought process is shown in Figures 2 and 3. Figure 2 shows that, regardless of whether $S_{i,s}$ is greater than or less than zero, the mechanism ensures that $S_{i,s}$ approaches zero. Building on this process, Figure 3 provides a more detailed analyses derived from Figure 2. These figures demonstrate that the proposed mechanism, in various scenarios, ensures the optimal iteration of $\chi_{i,s}$, and leads to a more stable $S_{i,s}$ approaching zero, thereby improving control accuracy.

Remark 6. Through a comprehensive analysis of all possible scenarios and the application of the gradient descent concept, the self-correction mechanism is designed to ensure control precision while effectively reducing over-compensation issues.

3 Consensus tracking control design

An enhanced event-triggered cooperative learning strategy, incorporating both the encoding-decoding mechanism and the self-correction mechanism with an amendment function, is proposed.

Step 1. Because the encryption function is applied to system (1) in this paper, the synchronization error can be rewritten as

$$z_{i,1} = \sum_{j=1}^{N} a_{ij}(\beta_{i,1} - \beta_{j,1}) + b_i(\beta_{i,1} - y_r), \tag{16}$$

where $y_r = y_c + \hbar_{y_c}$ represents the leader signal after applying the encryption function. This ensures effective protection of the leader signal's information.

The transformed error is defined as $S_{i,1} = z_{i,1} - \xi_{i,1}$. $\xi_{i,1}$ is the compensating signal with $\xi_{i,1}(0) = 0$. Furthermore, the compensating signal $\xi_{i,1}$ is

$$\dot{\xi}_{i,1} = \delta_i(\bar{\alpha}_{i,2} - \alpha_{i,1}) + \delta_i \breve{\hbar}_{i,1}\dot{\hbar}_{i,1} - b_i \breve{\hbar}_{i,1}\dot{\hbar}_{y_c} - \delta_i k_{i,1}\xi_{i,1} + \delta_i \xi_{i,2} - \frac{\ell_{i,1}\xi_{i,1}}{\sqrt{\xi_{i,1}^2 + \sigma_{i,1}^2}} - \sum_{j=1}^{N} a_{ij}\breve{\hbar}_{j,1}\dot{\hbar}_{j,1}, \tag{17}$$

where $k_{i,\flat}$ and $\ell_{i,\flat}$ are known positive constants. The parameter $\sigma_{i,\flat}$ must satisfy $\lim_{t\to\infty}\int_{t_0}^{t}\sigma_{i,\flat}(s)\mathrm{d}s \leqslant \bar{\sigma}_{i,\flat} < \infty$, where $\bar{\sigma}_{i,\flat}$ is a positive constant.

Remark 7. By leveraging command filtering technology, the terms $\delta_i\breve{\hbar}_{i,1}\dot{\hbar}_{i,1}$, $\sum_{j=1}^{N} a_{ij}\breve{\hbar}_{j,1}\dot{\hbar}_{j,1}$ and $b_i\breve{\hbar}_{i,1}\dot{\hbar}_{y_c}$ are incorporated into the filtering compensation signal. These terms effectively compensate for the corresponding variables in $\dot{z}_{i,1}$, thereby facilitating the decoding of the encrypted data.

The Lyapunov function is defined as $\mathcal{V}_{i,1} = \frac{1}{2}S_{i,1}^2 + \frac{1}{2}\tilde{\vartheta}_{i,1}^2$. The derivative of $S_{i,1}$ is given by

$$\begin{aligned}\dot{S}_{i,1} = {} & \delta_i S_{i,2} + \delta_i\alpha_{i,1} + \delta_i\varphi_{i,1} + \delta_i\breve{D}_{i,1} - \sum_{j=1}^{N} a_{ij}[\beta_{j,2} + \varphi_{j,1} + \breve{D}_{j,1}] - b_i\dot{y}_c + \delta_i k_{i,1}\xi_{i,1} \\ & + \frac{\ell_{i,1}\xi_{i,1}}{\sqrt{\xi_{i,1}^2 + \sigma\xi_{i,1}^2}} + \breve{\nu}_{i,1},\end{aligned} \tag{18}$$

where $\breve{\nu}_{i,1} = \delta_i(1-\breve{\hbar}_{i,1})\dot{\hbar}_{i,1} - \sum_{j=1}^{N} a_{ij}(1-\breve{\hbar}_{j,1})\dot{\hbar}_{j,1} - b_i(1-\breve{\hbar}_{i,1})\dot{\hbar}_{y_c}$. This function is bounded, satisfying $\breve{\nu}_{i,1} < \breve{\epsilon}_{i,1}$.

Based on this, the derivative of $\mathcal{V}_{i,1}$ is given by

$$\begin{aligned}\dot{\mathcal{V}}_{i,1} = {} & S_{i,1}\Bigg[\delta_i S_{i,2} + \delta_i\alpha_{i,1} + \delta_i\varphi_{i,1} + \delta_i\breve{D}_{i,1} - \sum_{j=1}^{N} a_{ij}[\beta_{j,2} + \varphi_{j,1} + \breve{D}_{j,1}] - b_i\dot{y}_c + \delta_i k_{i,1}\xi_{i,1} \\ & + \frac{\ell_{i,1}\xi_{i,1}}{\sqrt{\xi_{i,1}^2 + \sigma_{i,1}^2}} + \breve{\nu}_{i,1}\Bigg] - \tilde{\vartheta}_{i,1}^{\mathrm{T}}\dot{\hat{\vartheta}}_{i,1}.\end{aligned} \tag{19}$$

The FLSs are utilized to estimate $\varphi_{i,1}$, which can be expressed as

$$\varphi_{i,1} = \vartheta_{i,1}^{\mathrm{T}}\Xi_{i,1} + \epsilon_{i,1}, \tag{20}$$

where $\epsilon_{i,1}$ represents the approximation error.

The virtual control signal is designed as

$$\begin{aligned}\alpha_{i,1} = {} & -k_{i,1}S_{i,1} - q_{i,1}S_{i,1} - k_{i,1}\xi_{i,1} - \frac{\ell_{i,1}\xi_{i,1}}{\sqrt{\xi_{i,1}^2 + \sigma_{i,1}^2}} - \frac{1}{\delta_i}\hat{\vartheta}_{i,1}^{\mathrm{T}}\Xi_{i,1} \\ & - \hat{\breve{D}}_{i,1} + \frac{\sum_{j=1}^{N} a_{ij}}{\delta_i}(\beta_{j,2} + \hat{\breve{D}}_{j,1}) + \frac{b_i}{\delta_i}\dot{y}_c,\end{aligned} \tag{21}$$

where $q_{i,\flat}$ is a constant, and $\hat{\vartheta}_{i,\flat}$ is an estimate of $\vartheta_{i,\flat}$ with $\tilde{\vartheta}_{i,\flat} = \vartheta_{i,\flat} - \hat{\vartheta}_{i,\flat}$.

Substituting (21) into (19) yields

$$\begin{aligned}\dot{\mathcal{V}}_{i,1} = {} & \delta_i S_{i,1}S_{i,2} - \delta_i k_{i,1}S_{i,1}^2 - q_{i,1}\delta_i S_{i,1}^2 + S_{i,1}\tilde{\vartheta}_{i,1}^{\mathrm{T}}\Xi_{i,1} + \delta_i S_{i,1}\epsilon_{i,1} + \delta_i\tilde{\breve{D}}_{i,1}S_{i,1} \\ & - \tilde{\vartheta}_{i,1}^{\mathrm{T}}\dot{\hat{\vartheta}}_{i,1} + S_{i,1}\breve{\epsilon}_{i,1} + \sum_{j=1}^{N} a_{ij}\tilde{\breve{D}}_{j,1}S_{i,1}.\end{aligned} \tag{22}$$

The adaptive law is

$$\dot{\hat{\vartheta}}_{i,1} = \Xi_{i,1}S_{i,1} - \rho_{i,1}\hat{\vartheta}_{i,1}, \tag{23}$$

where $\rho_{i,\flat}$ is the designed parameter. Based on Young's inequality, it can be rearranged as

$$\dot{\mathcal{V}}_{i,1} \leqslant -\left[\delta_i(k_{i,1}+q_{i,1}) - \frac{3}{2}\delta_i^2 - 1\right] S_{i,1}^2 + \frac{1}{2}S_{i,2}^2 - \frac{\rho_{i,1}}{2}\tilde{\vartheta}_{i,1}^{\mathrm{T}}\tilde{\vartheta}_{i,1} + C_{i,1}, \tag{24}$$

where $C_{i,1} = \frac{1}{2}\bar{\epsilon}_{i,1}^2 + \frac{1}{2}\check{\epsilon}_{i,1}^2 + \frac{1}{2}\varrho_{\tilde{\check{D}}_{i,1}}^2 + \frac{1}{2}[\sum_{j=1}^{N} a_{ij}\varrho_{\tilde{\check{D}}_{j,1}}]^2 + \frac{\rho_{i,1}}{2}\vartheta_{i,1}^{*\mathrm{T}}\vartheta_{i,1}^*$. $\tilde{\check{D}}_{\bullet,1}$ is bounded with $|\tilde{\check{D}}_{\bullet,1}| < \varrho_{\tilde{\check{D}}_{\bullet,1}}$, and a detailed description is provided in [27].

Step $\acute{\lambda}$ $(\acute{\lambda} = 2, \ldots, n-1)$**.** The synchronization error is defined as $z_{i,\acute{\lambda}} = \beta_{i,\acute{\lambda}} - \bar{\alpha}_{i,\acute{\lambda}}$. Thus, $\dot{z}_{i,\acute{\lambda}}$ becomes

$$\dot{z}_{i,\acute{\lambda}} = \beta_{i,\acute{\lambda}+1} + \varphi_{i,\acute{\lambda}} + \dot{\hbar}_{i,\acute{\lambda}} + \check{D}_{i,\acute{\lambda}} - \dot{\bar{\alpha}}_{i,\acute{\lambda}}. \tag{25}$$

Next, the transformation of coordinates is defined as $S_{i,\acute{\lambda}} = z_{i,\acute{\lambda}} - \xi_{i,\acute{\lambda}}$, where $\xi_{i,\acute{\lambda}}$ is the compensating signal, which is constructed as

$$\dot{\xi}_{i,\acute{\lambda}} = \bar{\alpha}_{i,\acute{\lambda}+1} - \alpha_{i,\acute{\lambda}} + \check{\hbar}_{i,\acute{\lambda}}\dot{\hbar}_{i,\acute{\lambda}} - k_{i,\acute{\lambda}}\xi_{i,\acute{\lambda}} + \xi_{i,\acute{\lambda}+1} - \frac{\ell_{i,\acute{\lambda}}\xi_{i,\acute{\lambda}}}{\sqrt{\xi_{i,\acute{\lambda}}^2 + \sigma_{i,\acute{\lambda}}^2}}. \tag{26}$$

The Lyapunov function is defined as

$$\mathcal{V}_{i,\acute{\lambda}} = \frac{1}{2}S_{i,\acute{\lambda}}^2 + \frac{1}{2}\tilde{\vartheta}_{i,\acute{\lambda}}^2. \tag{27}$$

The FLSs are utilized to estimate $\varphi_{i,\acute{\lambda}}$. Thus, it can be expressed as

$$\varphi_{i,\acute{\lambda}} = \vartheta_{i,\acute{\lambda}}^{\mathrm{T}}\Xi_{i,\acute{\lambda}} + \epsilon_{i,\acute{\lambda}}. \tag{28}$$

The virtual control signal and adaptive law are designed as

$$\alpha_{i,\acute{\lambda}} = -k_{i,\acute{\lambda}}S_{i,\acute{\lambda}} - q_{i,\acute{\lambda}}S_{i,\acute{\lambda}} - k_{i,\acute{\lambda}}\xi_{i,\acute{\lambda}} - \frac{\ell_{i,\acute{\lambda}}\xi_{i,\acute{\lambda}}}{\sqrt{\xi_{i,\acute{\lambda}}^2 + \sigma_{i,\acute{\lambda}}^2}} - \frac{1}{\delta_i}\hat{\vartheta}_{i,\acute{\lambda}}^{\mathrm{T}}\Xi_{i,\acute{\lambda}} - \hat{\check{D}}_{i,\acute{\lambda}} + \frac{\alpha_{i,\acute{\lambda}-1} - \bar{\alpha}_{i,\acute{\lambda}}}{\upsilon_{i,\acute{\lambda}}}, \tag{29}$$

$$\dot{\hat{\vartheta}}_{i,\acute{\lambda}} = \Xi_{i,\acute{\lambda}}S_{i,\acute{\lambda}} - \rho_{i,1}\hat{\vartheta}_{i,\acute{\lambda}}. \tag{30}$$

Based on Young's inequality, the adaptive law $\dot{\hat{\vartheta}}_{i,\acute{\lambda}}$ and the virtual control signal $\alpha_{i,\acute{\lambda}}$, $\dot{\mathcal{V}}_{i,\acute{\lambda}}$ can be rewritten as

$$\dot{\mathcal{V}}_{i,\acute{\lambda}} = -\left[\delta_i k_{i,1} - \frac{3}{2}\delta_i^2 - 1\right] S_{i,1}^2 + \frac{1}{2}S_{i,\acute{\lambda}+1}^2 - \sum_{p=1}^{\acute{\lambda}}\left(k_{i,p} + q_{i,p} - \frac{5}{2}\right) S_{i,p}^2 - \sum_{p=1}^{\acute{\lambda}}\frac{\rho_{i,p}}{2}\tilde{\vartheta}_{i,p}^{\mathrm{T}}\tilde{\vartheta}_{i,p} + C_{i,\acute{\lambda}}, \tag{31}$$

where $C_{i,\acute{\lambda}} = C_{i,\acute{\lambda}-1} + \frac{1}{2}\bar{\epsilon}_{i,\acute{\lambda}}^2 + \frac{1}{2}\varrho_{\tilde{\check{D}}_{i,\acute{\lambda}}} + \frac{\rho_{i,\acute{\lambda}}}{2}\vartheta_{i,\acute{\lambda}}^{*\mathrm{T}}\vartheta_{i,\acute{\lambda}}^*$.

Step n**.** Define $z_{i,n} = \beta_{i,n} - \bar{\alpha}_{i,n}$, $R_{i,n} = \beta_{i,n} - \alpha_{i,n-1}$ and $S_{i,n} = z_{i,n} - \xi_{i,n}$. Thus, $\dot{z}_{i,n}$ and $\dot{\xi}_{i,n}$ are represented as

$$\dot{z}_{i,n} = -\mathfrak{u}_i + \varphi_{i,n} + \dot{\hbar}_{i,n} + \check{D}_{i,n} - \dot{\bar{\alpha}}_{i,n}, \tag{32}$$

$$\dot{\xi}_{i,n} = -k_{i,n}\xi_{i,n} + \check{\hbar}_{i,n}\dot{\hbar}_{i,n} - \frac{\ell_{i,n}\xi_{i,n}}{\sqrt{\xi_{i,n}^2 + \sigma_{i,n}^2}}. \tag{33}$$

Let $\bar{\varphi}_{i,n} = \varphi_{i,n} - q_{i,n}R_{i,n}$. The FLSs are used to handle $\bar{\varphi}_{i,n}$, yielding

$$\bar{\varphi}_{i,n} = \vartheta_{i,n}^*\Xi_{i,n} + \epsilon_{i,n}. \tag{34}$$

Choose the Lyapunov function as $V_{i,n} = V_{i,n-1} + \frac{1}{2}S_{i,n}^2 + \frac{1}{2}\tilde{\vartheta}_{i,n}^2$. $\dot{V}_{i,n}$ can be represented as

$$\dot{\mathcal{V}}_{i,n} \leqslant -\left[\delta_i(k_{i,1}+q_{i,1}) - \frac{3}{2}\delta_i^2 - 1\right] S_{i,1}^2 + \frac{1}{2}S_{i,n}^2 - \sum_{p=1}^{n-1}\frac{\rho_{i,p}}{2}\tilde{\vartheta}_{i,p}^{\mathrm{T}}\tilde{\vartheta}_{i,p} - \sum_{p=1}^{n-1}\left(k_{i,p} + q_{i,p} - \frac{5}{2}\right) S_{i,p}^2 + C_{i,n-1}$$

$$+ S_{i,n}\left[\mathfrak{u}_i + \vartheta_{i,n}^{*}\Xi_{i,n} + \epsilon_{i,n} + q_{i,n}R_{i,n} + \breve{D}_{i,n} - \dot{\bar{\alpha}}_{i,n} + k_{i,n}\xi_{i,n} + \frac{\ell_{i,n}\xi_{i,n}}{\sqrt{\xi_{i,n}^2+\sigma_{i,n}^2}}\right] - \tilde{\vartheta}_{i,n}^{\mathrm{T}}\dot{\hat{\vartheta}}_{i,n}. \tag{35}$$

The control signal is defined as

$$\mathfrak{u}_i = -k_{i,n}S_{i,n} - q_{i,n}R_{i,n} - k_{i,n}\xi_{i,n} - \frac{\ell_{i,n}\xi_{i,n}}{\sqrt{\xi_{i,n}^2+\sigma_{i,n}^2}} - \hat{\vartheta}_{i,n}^{\mathrm{T}}\Xi_{i,n} - \hat{\breve{D}}_{i,n} + \dot{\bar{\alpha}}_{i,n}. \tag{36}$$

To reduce the communication burden between signals, each piece of information is transmitted intermittently to its neighbors, using the switching threshold strategy

$$t_{k_i+1}^{i} = \begin{cases} \inf\{t\in\mathbb{R}^{+}|\acute{\mathcal{I}}_{i,n}(t)\geqslant 0\}, & \parallel \hat{\vartheta}_{i,n}(t)\parallel < \phi_{i,n}, \\ \inf\{t\in\mathbb{R}^{+}|\breve{\mathcal{I}}_{i,n}(t)\geqslant 0\}, & \parallel \hat{\vartheta}_{i,n}(t)\parallel \geqslant \phi_{i,n}. \end{cases}$$

Let $e_{i,\vartheta n} = \hat{\vartheta}_{i,n}(t_{k_i}^{i}) - \hat{\vartheta}_{i,n}(t)$. The triggering functions are defined as

$$\begin{cases} \acute{\mathcal{I}}_{i,n}(t) = \mathrm{e}^{|S_{i,n}|}\parallel e_{i,\vartheta n}\parallel - \varsigma_{i,n}\parallel \hat{\vartheta}_{i,n}(t)\parallel - \mathrm{csch}(w_{i,n}|S_{i,n}| + \acute{w}_{i,n}) - \Theta_{i,n}, \\ \breve{\mathcal{I}}_{i,n}(t) = \mathrm{e}^{|S_{i,n}|}\parallel e_{i,\vartheta n}\parallel - \varsigma_{i,n}\phi_{i,n} - \mathrm{csch}(\acute{w}_{i,n}) - \Theta_{i,n}, \end{cases}$$

where $\varsigma_{i,n} < 1$. $\phi_{i,n}$, $w_{i,n}$, $\acute{w}_{i,n}$ and $\Theta_{i,n}$ are positive designed parameters.

Therefore, the adaptive law is defined as

$$\dot{\hat{\vartheta}}_{i,n} = S_{i,n}\Xi_{i,n} - \rho_{i,n}\hat{\vartheta}_{i,n} - \gamma_{i,n}\sum_{j=1}^{N} a_{ij}[\hat{\vartheta}_{i,n}(t_{k_i}^{i}) - \hat{\vartheta}_{j,n}(t_{k_j}^{j})], \tag{37}$$

where the proof for excluding Zeno behavior follows a similar approach to [23]. By incorporating neighbor information into the adaptive law, the robustness of the control strategy is enhanced through the adaptive laws of neighboring nodes. Additionally, to reduce the unnecessary communication burden in the cooperative learning strategy, a switching event-triggered strategy is introduced in the adaptive law framework.

Remark 8. Inspired in part by [23], this paper presents a cooperative learning strategy in the adaptive law framework. It is important to note that the trigger condition takes both the trigger error and system performance into account, effectively reducing unnecessary communication burden while ensuring control performance.

In light of Young's inequality, (36) and (37), the following holds:

$$\begin{aligned} \dot{\mathcal{V}}_{i,n} \leqslant & -\left[\delta_i k_{i,1} - \frac{3}{2}\delta_i^2 - 1\right] S_{i,1}^2 - \sum_{p=1}^{n-1}\frac{\rho_{i,p}}{2}\tilde{\vartheta}_{i,p}^{\mathrm{T}}\tilde{\vartheta}_{i,p} - \sum_{p=2}^{n-1}\left(k_{i,p} + q_{i,p} - \frac{5}{2}\right) S_{i,p}^2 + C_{i,n} \\ & - \left(k_{i,n} - \frac{3}{2}\right) S_{i,n}^2 - \left[\left(\rho_{i,n} + \gamma_{i,n}\sum_{j=1}^{N} a_{ij}\right) - 1\right]\tilde{\vartheta}_{i,n}^{\mathrm{T}}\tilde{\vartheta}_{i,n}, \end{aligned} \tag{38}$$

where $C_{i,n} = \frac{1}{2}\varrho_{\tilde{\breve{D}}_{i,n}}^2 + \frac{1}{4}(\rho_{i,n} + \gamma_{i,n}\sum_{j=1}^{N} a_{ij})\ \vartheta_{i,n}^{*\mathrm{T}}\vartheta_{i,n}^{*} + \frac{1}{2}e_{i,\vartheta n}^2 + \frac{1}{2}[\gamma_{i,n}\sum_{j=1}^{N} a_{ij}]^2\hat{\vartheta}_{j,n}^{\mathrm{T}}(t_{k_j}^{j})\hat{\vartheta}_{j,n}(t_{k_j}^{j}) + \frac{1}{2}\bar{\epsilon}_{i,n}^2$, $\delta_i k_{i,1} > \frac{3}{2}\delta_i + 1$, $k_{i,p} + q_{i,p} > \frac{5}{2}$ and $k_{i,n} > \frac{3}{2}$.

Let $\wp_i = \min\{[\delta_i k_{i,1} - \frac{3}{2}\delta_i^2 - 1], (k_{i,p} + q_{i,p} - \frac{5}{2}), (k_{i,n} - \frac{3}{2}), \frac{\rho_{i,s}}{2}, [(\rho_{i,n} + \gamma_{i,n}\sum_{j=1}^{N} a_{ij}) - 1]\}$ and $\Im_i = C_{i,n}$. Therefore, it follows that

$$\dot{\mathcal{V}}_{i,n} \leqslant -\wp_i V_{i,n} + \Im_i. \tag{39}$$

4 Stability analysis

This section presents the proof process for the stability analysis. Additionally, to ensure the completeness of the theoretical proof, the boundedness of the compensation signal and the estimation error will be demonstrated.

4.1 Proof of stability analysis

Theorem 1. Based on MASs, the desired control objective can be achieved by combining the controllers (21), (29) and (36) with the adaptive laws (23), (30) and (37).

Proof. Let the Lyapunov function be defined as

$$\bar{\mathcal{V}} = \sum_{i=1}^{N} \mathcal{V}_{i,n}. \tag{40}$$

This leads to the inequality

$$\dot{\bar{V}} \leqslant -\breve{\wp}\bar{\mathcal{V}} + \breve{\Im}, \tag{41}$$

where $\breve{\wp} = \min\{\varpi_i, i = 1, 2, \ldots, N\}$ and $\breve{\Im} = \sum_{i=1}^{N} \Im_i$. Inspired by [41], this ensures that the first control objective is achieved.

After analysis, it follows that

$$0 \leqslant \bar{\mathcal{V}}(t) \leqslant \mathrm{e}^{-\breve{\wp}t}\bar{\mathcal{V}}(0) + \frac{\breve{\Im}}{\breve{\wp}}(1 - \mathrm{e}^{-\breve{\wp}t}). \tag{42}$$

Furthermore, it can be derived that

$$\| S_{i,1} \|^2 \leqslant 2\mathrm{e}^{-\breve{\wp}t}\bar{\mathcal{V}}(0) + \frac{2\breve{\Im}}{\breve{\wp}}(1 - \mathrm{e}^{-\breve{\wp}t}). \tag{43}$$

Based on Lemma 2 and (43), the tracking error $\| \bar{y}_i - \bar{y}_r \|$ can converge to a small residual concentration.

4.2 Proof of boundedness for the compensation signal

Based on command filtering technology, it is necessary to prove that the compensation signal remains bounded. The detailed proof process is as follows. Inspired in part by [37], we assumed that $\| \bar{\alpha}_{i,p+1} - \alpha_{i,p} \| \leqslant \acute{\varepsilon}_{i,p}$ is bounded and satisfies $\| \bar{\alpha}_{i,p+1} - \alpha_{i,p} \| \leqslant \varepsilon_{i,p}$ with $p = 1, 2, \ldots, n-1$.

The Lyapunov function is

$$\mathcal{V}_{n+1} = \sum_{p=1}^{n} \frac{1}{2}\xi_{i,p}^2. \tag{44}$$

According to Lemma 4 and Young's inequality, it follows that

$$\begin{aligned}
\dot{\mathcal{V}}_{n+1} \leqslant & -\left[(d_i + b_i)k_{i,1} - \frac{1}{2}(d_i + b_i)^2\right]\xi_{i,1}^2 - \left[\sum_{p=2}^{n-1} k_{i,p} - 1\right]\xi_{i,p}^2 - \left(k_{i,n} - \frac{1}{2}\right)\xi_{i,n}^2 - \Bigg[\ell_{i,1} - (d_i + b_i)\acute{\varepsilon}_{i,1} \\
& - (d_i + b_i)|\breve{\hbar}_{i,1}\dot{\hbar}_{i,1}| - \sum_{j=1}^{N} a_{ij}|\breve{\hbar}_{j,1}\dot{\hbar}_{j,1}| - b_i|\breve{\hbar}_{i,1}\dot{\hbar}_{y_c}|\Bigg]|\xi_{i,1}| - \sum_{p=2}^{n}[\ell_{i,p} - |\breve{\hbar}_{i,p}\dot{\hbar}_{i,p}| - \acute{\varepsilon}_{i,p}]|\xi_{i,p}| \\
& + \sum_{p=1}^{n} \ell_{i,p}\vec{\kappa}_{i,p}.
\end{aligned} \tag{45}$$

Based on the abovementioned analyses, the compensation signal is bounded if $\ell_{i,1} > (d_i + b_i)\acute{\varepsilon}_{i,1} + (d_i + b_i)|\breve{\hbar}_{i,1}\dot{\hbar}_{i,1}| + \sum_{j=1}^{N} a_{ij}|\breve{\hbar}_{j,1}\dot{\hbar}_{j,1}| + b_i|\breve{\hbar}_{i,1}\dot{\hbar}_{y_c}|$ and $\ell_{i,p} > |\breve{\hbar}_{i,p}\dot{\hbar}_{i,p}| + \acute{\varepsilon}_{i,p}$.

4.3 Proof of boundedness for the estimation error

This subsection proves that the estimation error is bounded.

We select the Lyapunov function as $\bar{\mathcal{V}}_i = \sum_{p=1}^{n} \frac{1}{2}\tilde{\nu}_{i,s}^2$. Then, $\dot{\bar{\mathcal{V}}}_i$ is expressed as

$$\dot{\bar{\mathcal{V}}}_i = \sum_{p=1}^{n} \frac{1}{2}\tilde{\nu}_{i,p}[\dot{\nu}_{i,p} - \dot{\hat{\nu}}_{i,p}]. \tag{46}$$

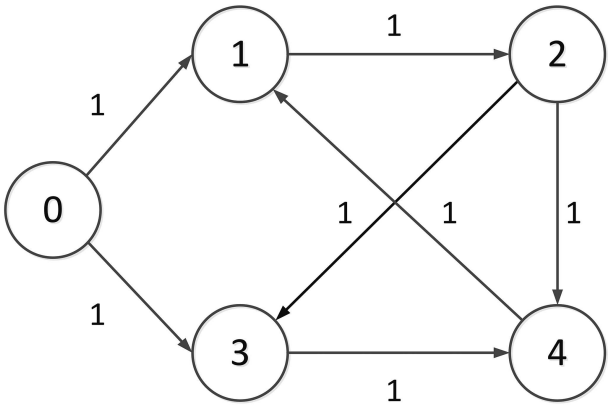

Figure 4 Communication topology.

According to Young's inequality, (12) and (14), one has

$$\dot{\mathcal{V}}_i \leqslant \sum_{p=1}^{n} \left(G_{i,p} - \mu_{i,p}\chi_{i,p}\eta_{i,p} + \frac{1}{2} \right) \tilde{\nu}_{i,p}^2 + \sum_{p=1}^{n} \frac{1}{2} [\vec{\zeta}_{i,p}]^2. \tag{47}$$

By appropriately adjusting the value of $\mu_{i,p}$, it can ensure that $(G_{i,p} - \mu_{i,p}\chi_{i,p}\eta_{i,p} + \frac{1}{2})$ is always negative. This guarantees that the estimation error $\tilde{\nu}_{i,p}$ remains bounded.

5 Simulation results

This section demonstrates the effectiveness of the proposed scheme using an example of a single torsion pendulum system [42]. The form is as follows:

$$\begin{aligned} &\frac{\partial \vec{\hbar}_i}{\partial t} = \omega_i, \\ &J_i \frac{\partial \vec{\hbar}_i}{\partial t} = u_i - M_i g_i l_i \sin(\vec{\hbar}_i) - f_{d,i} \frac{\partial \vec{\hbar}_i}{\partial t}. \end{aligned} \tag{48}$$

The parameters in (48) are provided in [42], and the mathematical model is given as

$$\begin{aligned} &\dot{x}_{i,1} = x_{i,2}, \\ &\dot{x}_{i,2} = J_i^{-1}\big(- M_i g_i l_i \sin(x_{i,1}) - f_{d,i} x_{i,1} \big) + J_i^{-1} u_i + \breve{D}, \end{aligned} \tag{49}$$

where $\breve{D}$ represents the disturbance.

Additionally, the leader signal is given by $y_c = 4\sin(t)$.

In sight of Figure 4, the adjacency matrix is $A = [0\ 0\ 0\ 1;\ 1\ 0\ 0\ 0;\ 0\ 1\ 0\ 0;\ 0\ 1\ 1\ 0]$.

Let $\mathbb{B} = \mathrm{diag}(1, 0, 1, 0)$. Furthermore, the initial values are $x_{1,1}(0) = x_{3,1}(0) = x_{4,1}(0) = -0.3$, $x_{2,1}(0) = 0.2$, $x_{1,2}(0) = 0$, $x_{2,2}(0) = x_{3,2}(0) = x_{4,2}(0) = 0.1$, $\tau_{i,1}(0) = \tau_{i,2}(0) = 0.1$, $\hat{\nu}_{i,1}(0) = \hat{\nu}_{i,2}(0) = 0.1$, $\chi_{i,\flat}(0) = 1$ and $\hat{\vartheta}_{i,1}(0) = \hat{\vartheta}_{i,2}(0) = [0.2, \ldots, 0.2]^{\mathrm{T}} \in \mathbb{R}^{5\times 1}$, where $i = 1, 2, 3, 4$ and $\flat = 1, 2$.

The designed parameters are $k_{i,1} = 350$, $k_{i,2} = 480$, $q_{i,1} = 80$, $q_{i,2} = 100$, $\ell_{i,\flat} = 29$, $\upsilon_{i,1} = 40$, $\upsilon_{i,2} = 50$, $G_{i,\flat} = 0.2$, $\eta_{i,\flat} = 0.5$, $\iota_{i,\flat} = 2$, $\breve{\iota}_{i,\flat} = 1.5$, $\aleph_{i,\flat} = 3$, $\aleph_{2,1} = 4$, $\rho_{i,\flat} = 0.1$, $\mu_{i,\flat} = 1$, $\phi_{i,2} = 1$, $\varsigma_{i,2} = 0.5$, $\nabla_{i,\flat} = 10$, $\breve{w}_{i,\flat} = 1$, $\breve{\upsilon}_{i,1} = 13$, $\breve{\upsilon}_{i,2} = 8$ and $\acute{w}_{i,2} = \Theta_{i,2} = \Theta_{i,2} = \gamma_{i,2} = 1$.

Figure 5 clearly shows that the followers are able to track the reference signal. As observed from the trajectories in Figures 6–8, there is a deviation between the encrypted information and the actual information, which prevents malicious agents from stealing sensitive data. Therefore, Figures 6–8 show that the information of the agent is effectively protected. Figure 9 shows that the proposed self-correction mechanism, compared to [27], enhances the tracking performance of the system. Meanwhile, the trajectories of the self-correction mechanism are shown in Figure 10, demonstrating that the final trajectories converge to a local optimum. Figure 11 shows the time intervals of the event-triggered strategy, while Figure 12 shows the trajectories of the adaptive laws. Based on these figures, the simulation results validate the effectiveness of the proposed scheme.

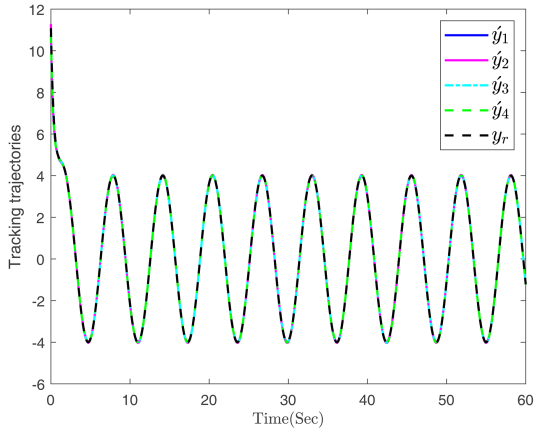

Figure 5 (Color online) Tracking trajectories with data protection.

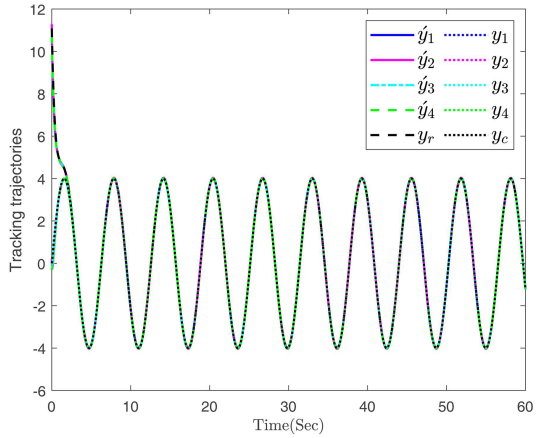

Figure 6 (Color online) Comparison of tracking trajectories.

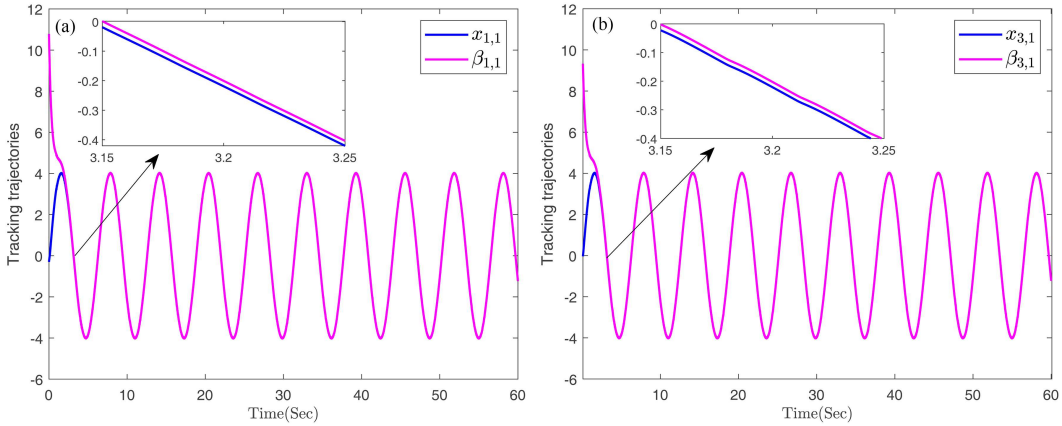

Figure 7 (Color online) State trajectories of the agents (first step) with (a) first agent and (b) second agent.

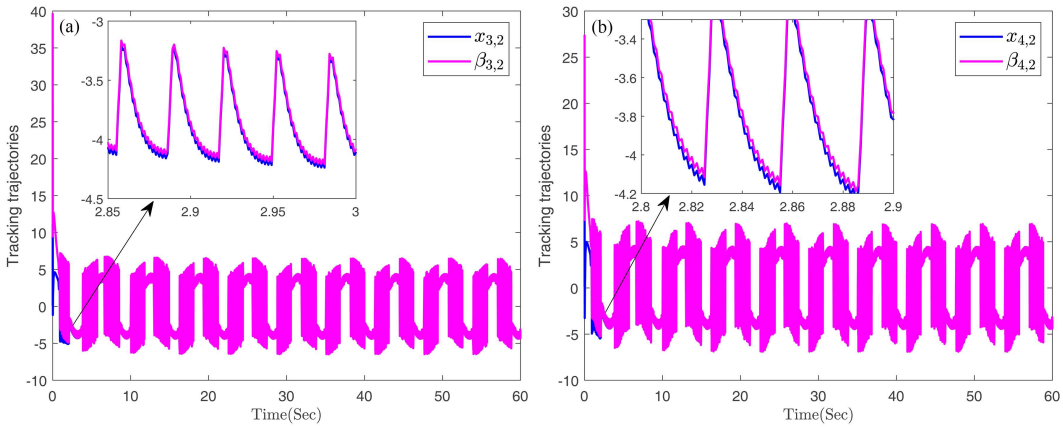

Figure 8 (Color online) State trajectories of the agents (second step) with (a) third agent and (b) fourth agent.

6 Conclusion

This paper presents a distributed cooperative learning control scheme featuring data protection and a self-correction mechanism. Using a mask function and command filtering technology, an encryption-decryption mechanism has been established to protect the sensitive information of the agent from detection by malicious agents, while minimizing the impact on system control performance. Additionally, based on the disturbance observer and the gradient descent approach, a self-correction mechanism has been proposed, addressing the issue of over-compensation for

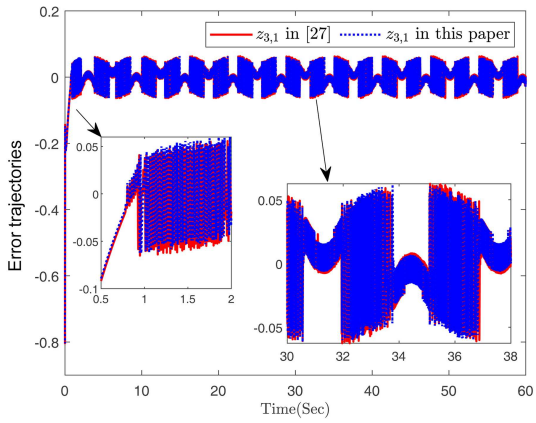

Figure 9 (Color online) Error trajectories of the third agent.

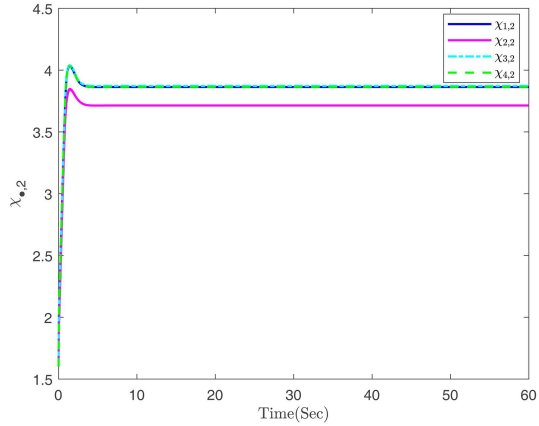

Figure 10 (Color online) Trajectories of the self-correction mechanism.

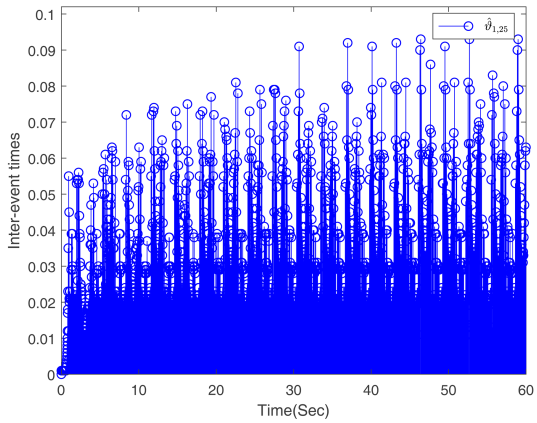

Figure 11 (Color online) Time intervals of the event-triggered strategy.

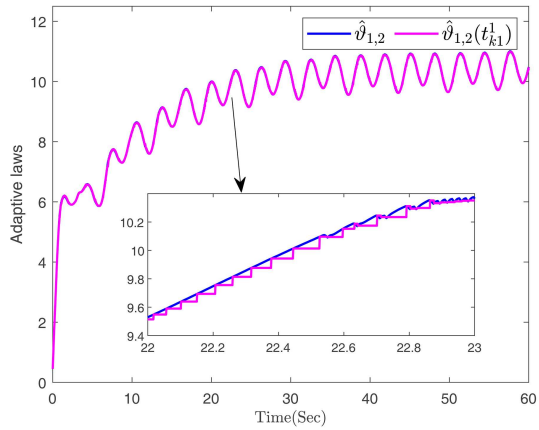

Figure 12 (Color online) Trajectories of the adaptive laws.

errors. Furthermore, a cooperative learning strategy has been incorporated into the adaptive laws to enhance the robustness of the system. The designed event-triggered condition effectively reduces unnecessary communication overhead without compromising control performance. The effectiveness of the proposed scheme has been validated through a practical simulation example.

Acknowledgements This work was supported in part by National Natural Science Foundation of China (Grant Nos. 62433018, 62033003).

References

1 Zhou Q, Ren Q, Ma H, et al. Model-free adaptive control for nonlinear systems under dynamic sparse attacks and measurement disturbances. IEEE Trans Circ Syst I, 2024, 71: 4731–4741
2 Yuan L, Jiang T, Li L H, et al. Robust cooperative multi-agent reinforcement learning via multi-view message certification. Sci China Inf Sci, 2024, 67: 142102
3 Zhang W, Huang Q, Wang X, et al. Bipartite consensus for quantization communication multi-agents systems with event-triggered random delayed impulse control. IEEE Trans Circ Syst I, 2025, 72: 1751–1762
4 Wang Z, Mu C, Hu S, et al. Modelling the dynamics of regret minimization in large agent populations: a master equation approach. In: Proceedings of the 31st International Joint Conference on Artificial Intelligence, 2022. 524–540
5 Liu Y, Chen X B, Mei Y F, et al. Observer-based boundary control for an asymmetric output-constrained flexible robotic manipulator. Sci China Inf Sci, 2022, 65: 139203
6 Liu X K, Zhang J F, Wang J. Differentially private consensus algorithm for continuous-time heterogeneous multi-agent systems. Automatica, 2020, 122: 109283
7 Altafini C. A system-theoretic framework for privacy preservation in continuous-time multiagent dynamics. Automatica, 2020, 122: 109253
8 Hu J, Sun Q, Wang R, et al. Privacy-preserving sliding mode control for voltage restoration of AC microgrids based on output mask approach. IEEE Trans Ind Inf, 2022, 18: 6818–6827
9 Wang A, Liu Y, Huang T. Event-triggered privacy-preserving average consensus for continuous-time multi-agent network systems. J Franklin Inst, 2022, 359: 4959–4975
10 Yang S F, Liang H J, Pan Y N, et al. Security control for air-sea heterogeneous multiagent systems with cooperative-antagonistic interactions: an intermittent privacy preservation mechanism. Sci China Tech Sci, 2025, 68: 1420402
11 Gao C, Wang Z, He X, et al. Fault-tolerant consensus control for multiagent systems: an encryption-decryption scheme. IEEE Trans Automat Contr, 2022, 67: 2560–2567

12 Zhu K, Wang Z, Han Q L, et al. Distributed set-membership fusion filtering for nonlinear 2-D systems over sensor networks: an encoding-decoding scheme. IEEE Trans Cybern, 2023, 53: 416–427
13 Wang X, Guang W, Huang T, et al. Optimized adaptive finite-time consensus control for stochastic nonlinear multiagent systems with non-affine nonlinear faults. IEEE Trans Automat Sci Eng, 2024, 21: 5012–5023
14 Zhang X M, Han Q L, Zhang B L, et al. Accumulated-state-error-based event-triggered sampling scheme and its application to H^{∞} control of sampled-data systems. Sci China Inf Sci, 2024, 67: 162206
15 Lei Y, Hua T, Wang Y W, et al. Robust output regulation of singularly perturbed systems by event-triggered output feedback. IEEE Trans Syst Man Cybern Syst, 2024, 54: 2104–2113
16 Liu Y, Yao X, Zhao W. Distributed neural-based fault-tolerant control of multiple flexible manipulators with input saturations. Automatica, 2023, 156: 111202
17 Zhou X Z, An J, He Y, et al. Improved stability criteria for delayed neural networks via time-varying free-weighting matrices and S-procedure. IEEE Trans Neural Netw Learn Syst, 2024, 35: 16945–16951
18 Chen W, Hua S, Zhang H. Consensus-based distributed cooperative learning from closed-loop neural control systems. IEEE Trans Neural Netw Learn Syst, 2015, 26: 331–345
19 Liu Z, Zhang H, Sun J, et al. All agents connectivity-preserving and error-based cooperative learning control with data-filter memory-based event-triggered strategy. IEEE Trans Automat Sci Eng, 2025, 22: 5566–5577
20 Yuan C, He H, Wang C. Cooperative deterministic learning-based formation control for a group of nonlinear uncertain mechanical systems. IEEE Trans Ind Inf, 2019, 15: 319–333
21 Dai S L, He S, Ma Y, et al. Distributed cooperative learning control of uncertain multiagent systems with prescribed performance and preserved connectivity. IEEE Trans Neural Netw Learn Syst, 2021, 32: 3217–3229
22 Gao F, Chen W, Li Z, et al. Neural network-based cooperative identification for a class of unknown nonlinear systems via event-triggered communication. IEEE Trans Syst Man Cybern Syst, 2021, 51: 1404–1413
23 Zuo R, Li Y, Lv M, et al. Learning-based distributed containment control for HFV swarms under event-triggered communication. IEEE Trans Aerosp Electron Syst, 2023, 59: 568–579
24 Lei Y, Wang Y W, Liu X K, et al. Semi-global bounded output regulation of linear two-time-scale systems with input saturation. IEEE Trans Circ Syst I, 2023, 70: 4560–4569
25 Wang S Y, Polyakov A, Li M, et al. Optimal rejection of bounded perturbations in linear leader-following consensus protocol: invariant ellipsoid method. Sci China Inf Sci, 2024, 67: 180202
26 Cui Y, Qiao J, Zhu Y, et al. Velocity-tracking control based on refined disturbance observer for gimbal servo system with multiple disturbances. IEEE Trans Ind Electron, 2022, 69: 10311–10321
27 Kong L, He W, Liu Z, et al. Adaptive tracking control with global performance for output-constrained MIMO nonlinear systems. IEEE Trans Automat Contr, 2023, 68: 3760–3767
28 He T, Wu Z. Iterative learning disturbance observer based attitude stabilization of flexible spacecraft subject to complex disturbances and measurement noises. IEEE-CAA J Autom Sin, 2021, 8: 1576–1587
29 Nair R R, Behera L. Robust adaptive gain higher order sliding mode observer based control-constrained nonlinear model predictive control for spacecraft formation flying. IEEE-CAA J Autom Sin, 2018, 5: 367–381
30 Shao J, Shi L, Cheng Y, et al. Asynchronous tracking control of leader-follower multiagent systems with input uncertainties over switching signed digraphs. IEEE Trans Cybern, 2022, 52: 6379–6390
31 Sun J, Ming Z. Cooperative differential game-based distributed optimal synchronization control of heterogeneous nonlinear multiagent systems. IEEE Trans Cybern, 2023, 53: 7933–7942
32 Peng X J, He Y, Liu Z, et al. Time-varying formation H_{∞} tracking control and optimization for delayed multi-agent systems with exogenous disturbances. IEEE Trans Automat Sci Eng, 2025, 22: 5637–5647
33 Zhou Q, Yin C, Ma H, et al. Prescribed performance bipartite consensus control for MASs under data-driven strategy. IEEE-CAA J Autom Sin, 2025, 12: 937–946
34 Zheng X H, Ma H, Zhou Q, et al. Neural-based prescribed-time consensus control for multiagent systems via dynamic memory event-triggered mechanism. Sci China Tech Sci, 2025, 68: 1320402
35 Zheng S P, Ma H, Ren H R, et al. Practically fixed-time adaptive consensus control for multiagent systems with prescribed performance. Sci China Tech Sci, 2012, 67: 3867–3876
36 Zhang H, Lewis F L, Qu Z. Lyapunov, adaptive, and optimal design techniques for cooperative systems on directed communication graphs. IEEE Trans Ind Electron, 2012, 59: 3026–3041
37 Li Y X. Command filter adaptive asymptotic tracking of uncertain nonlinear systems with time-varying parameters and disturbances. IEEE Trans Automat Contr, 2022, 67: 2973–2980
38 Pan Y N, Chen Y L, Liang H J. Event-triggered predefined-time control for full-state constrained nonlinear systems: a novel command filtering error compensation method. Sci China Tech Sci, 2024, 67: 2867–2880
39 Liu Z, Liu J, Zhang O, et al. Adaptive disturbance observer-based fixed-time tracking control for uncertain robotic systems. IEEE Trans Ind Electron, 2024, 71: 14823–14831
40 Liu Z, Lin X, Gao Y, et al. Fixed-time sliding mode control for DC/DC buck converters with mismatched uncertainties. IEEE Trans Circ Syst I, 2023, 70: 472–480
41 Yoo S J. Distributed consensus tracking for multiple uncertain nonlinear strict-feedback systems under a directed graph. IEEE Trans Neural Netw Learn Syst, 2013, 24: 666–672
42 Li Y X, Yang G H, Tong S. Fuzzy adaptive distributed event-triggered consensus control of uncertain nonlinear multiagent systems. IEEE Trans Syst Man Cybern Syst, 2019, 49: 1777–1786